Cogging torque calculations for a novel concept of a Transverse Flux Linear Free-Piston Generator

Alija Cosic*† and Chandur Sadarangani*

*Royal Institute of Technology, School of Electrical Engineering, Teknikringen 33, SE-100 44 Stockholm, SWEDEN,
Phone +46-(0)8-790-7976, Facsimile +46-(0)8-205268

Email:†alija.cosic@ee.kth.se

Abstract This paper investigates cogging force in a linear Transverse Flux Machine, TFM. 3D-FEM and 2D-FEM simulations has been performed and also two analytical methods have been applied. The analytical methods are based on the reluctant pressure method. Once the field distribution on the side of the tooth is known, the cogging force can be calculated by integrating the field. The agreement between the 2D-FEM and Conformal Mapping, CM, analytical method is good. However the 3D-FEM simulation results indicates a lower cogging force than the other two methods.

Keywords: Cogging force, CM-method, TFM

1. Introduction

Cogging force in an electrical machine generate losses. The cogging torque is also a source to the tooth vibrations and motor noise. In the free piston energy converter the cogging torque is not of relatively high importance. It is because of the high forces during acceleration [1]. However, in order to get an optimal machine design the cogging torque should be minimized.

The free piston energy converter can be used in many different areas e.g. as a stand alone generator unit on a farm. It's purpose, in this study, is however as the generating unit in an electric vehicle. As mentioned, the cogging force is one of the sources of noise in the machine and in the vehicle application the noise should be reduced. Although the combustion itself may generate more noise, the system design should be optimal with respect to the total noise.

In this paper the cogging force in the novel TFM linear machine has been analyzed. 3-D simulations of the topologies has been performed in order to determine the cogging force. The 3D simulations, however, are very time consuming. Because of this an analytical tool had to be developed in order to optimize the machine and reduce the cogging force in a reasonable time.

Here two methods proposed: conformal mapping and relative permeance model [3] [2], are applied and the cogging force has been investigated. Both methods are based on the flux density distribution on the side of the tooth. Once the flux density distribution is known, using magnetic pressure integration the cogging force can be calculated.

2. Machine layout

The novel TFM machine topology offers several possibilities in magnet and winding arrangements, e.g. the global winding design and the local winding design [5]. In the global winding design, which is the one analyzed in this paper, the windings are arranged as in a conventional machine where the winding is wound around the complete length of the machine.

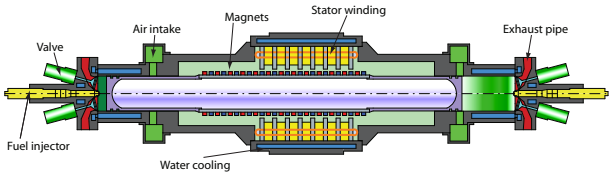

Fig. 1. Schematic view of the FPEC.

A cross sectional view of the machine, in axial direction, is shown in 2.

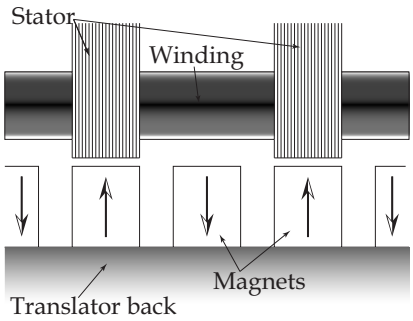

Fig. 2. Layout of the new TFM design

As can been seen from figure 2 there exist space between the stacks. This is something that resembles the pressure fingers in the big synchronous machines, in order to achieve a better cooling. In the case of the TFM, however, it is inherent in the working principle of the machine.

3. Relative permeance model

Usually the cogging torque/force is calculated with the energy method. However, due to the geometry of the machine, calculations of the permeance and final calculations of the energy change is a tedious task. In [2]an

alternative analytical method to the cogging force calculation is proposed. It is biased on the analytical calculation of the air gap field distribution.

Some of the assumptions needed, in order to simplify the magnetic field calculations are

- the magnetic field distribution, on the side of the tooth, is determined from the product of the magnetic field produced by the magnets and the relative permeance.
- The flux that crosses the air gap is assumed to follow a straight line just beneath the tooth and a circular line, centered about the corner of a tooth, in a slot opening.

Other assumptions are that the iron is infinitely permeable and the stator surface is smooth, i.e. there is no influence from the slot openings.

According to the theory, the reluctance pressure on the boundary between two regions [3], is given by

$$p_R = \frac{1}{2} \cdot (\mu_2 - \mu_1) \cdot \left(\frac{B_n^2}{\mu_1 \cdot \mu_2} + H_t^2 \right) \tag{1}$$

On the boundary the normal component of the magnetic induction B_n and tangential component of the magnetic field strength H_t are constant. Furthermore, if the permeability difference of the two boundary regions is big $\mu_2 \gg \mu_1$ then $H_t = 0$. The equation 2 then becomes

$$p_R = \frac{B_n^2}{2\mu_1} \tag{2}$$

The force equation is then given by integration of the reluctance pressure over the surface

$$\vec{F} = \int_S p_R d\vec{S} \tag{3}$$

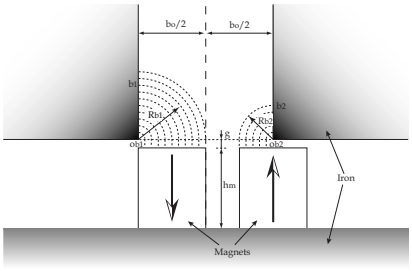

Fig. 3. Idealized flux path used for calculation of the permeance.

The cogging torque is calculated by assuming that the flux density distribution on the side of the tooth is the same as the flux density calculated at the stator bore radius at the slot opening and multiplied by the relative permeance of the assumed circular flux path.

$$\begin{aligned} F_{cog} &= \sum_{k=1}^{Q_s/3} w_{tooth} \int_{toothside} \left(\frac{B_{\theta b1}^2 - B_{\theta b1}^2}{2 \cdot \mu_0} \right) dy \\ &= \sum_{k=1}^{Q_s/3} w_{tooth} \int_0^{\frac{b_0}{2}} \left(\frac{B_{Rb1}^2 - B_{Rb2}^2}{2 \cdot \mu_0} \right) dy \end{aligned} \tag{4}$$

where w_{tooth} is the width of the tooth

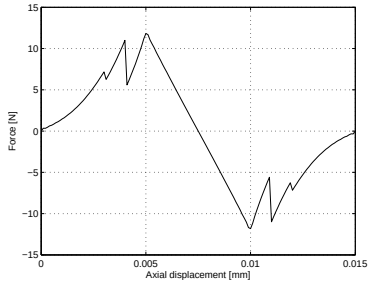

Fig. 4. Lateral force for one phase.

The assumption for the relative permeance model, that the flux follows a circular path centered about the corner of the tooth, needs in this case to be modified. It is only true if the the slot openings are narrow, compared to the pole length. In the case of the TFM, however, the space between the stacks is somewhat wider than the pole length. This means that one magnet will be in the middle of the two stack and will have no iron tooth just above. The flux from the magnet, that enters the side of the teeth, will no longer travel only in a circular path but more in an elliptical path. This has been modified in the model and it can also be seen in the results 4.

However, due to the wide space between the stacks these assumptions are somewhat insecure. The results will only give a hint of the magnitude.

4. Conformal Mapping CM

Conformal Mapping CM is a powerful analytical method that helps us to calculate 2D magnetic fields. The idea with the conformal mapping is to simplify a complex geometry in to a simple one, where the field, easily, can be calculated. The CM method has its roots in the complex analysis, where the complex geometry is placed in the complex plan z. Then, an analytical complex function $z = f(w)$, called the CM, is applied. This function will map lines or points into the new configuration placed in a new complex plane w.

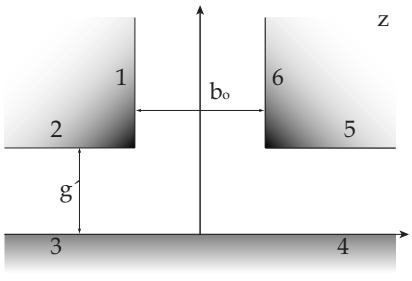

Fig. 5. Simplified TFM configuration in the z-plane.

It is also possible to perform several CM in a row until a simple enough configuration is obtained.

$$z = \frac{b_0}{\pi} \cdot \left[\arcsin\left(\frac{w}{a}\right) + \frac{g'}{b_0} \cdot \ln\left(\frac{\sqrt{a^2 - w^2} + \frac{2 \cdot g}{b_0} \cdot w}{\sqrt{a^2 - w^2} - \frac{2 \cdot g}{b_0} \cdot w} \right) \right] \tag{5}$$

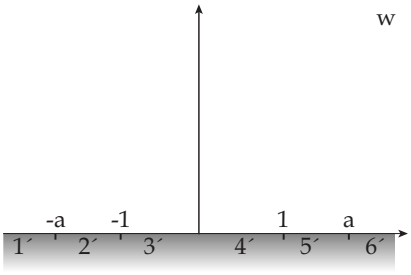

Fig. 6. Simplified TFM configuration in the w coordinate system.

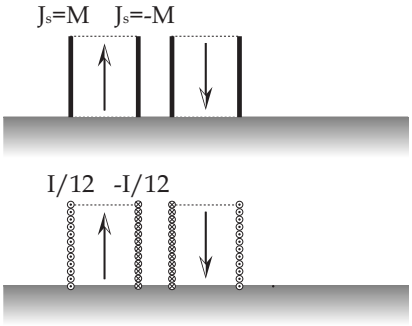

Fig. 7. Equivalent PM punctual currents.

where

$$a = \sqrt{1 + \left(\frac{2 \cdot g}{b_0}\right)} \quad (6) \text{ and } \quad g' = \frac{h_m}{\mu_r} \quad (7)$$

5. Equivalent current model

For modern magnetic materials the B-H characteristic in the second quadrant is a straight line [6]. It is given by the following equation

$$B = B_r + \mu \cdot H = B_r + \mu_0 \cdot \mu_r \cdot H \tag{8}$$

The magnetization is given by the following equation

$$M = \frac{B_r}{\mu_0} + (\mu_r - 1) \cdot H \tag{9}$$

For the NeFeB magnets the relative permeability varies between 1.03-1.07. In order to simplify calculations, the relative permeability μ_r,is assumed to be exactly 1. By choosing the relative permeability to 1 the second term in equation 9 vanishes, and the magnetization is constant for the whole PM body regardless of the field, so the equation becomes

$$M = \frac{B_r}{\mu_0} \tag{10}$$

It is possible to represent the magnetic field produced by the magnets with equivalent currents. According to [3], a magnet with magnetization $\vec{M}$ can be replaced by a system of two equivalent currents.

- The volume current with the density $\vec{J} = \nabla \times \vec{M}$
- The surface current with the density $\vec{J}_s = \vec{M} \cdot \vec{n}$, where $\vec{n}$ is a unit vector normal to the body surface.

These currents are placed in the air. Due to the fact that the PM magnetization in that magnet is constant, the volume current density is thus zero.

The magnetic field can then be represented by the equivalent surface currents that flows on the PM poles lateral sides, where vector $\vec{M}$ and $\vec{n}$ are normal. From this it follows that the equivalent surface current density is $J_s = \pm M$ and the total current flowing on the lateral side is [3]

$$I = J_s \cdot h_m = \pm M \cdot h_m \tag{11}$$

where the h_m is the height of the magnet.

In order to obtain the punctual currents, each of the surface currents is divided in to the n punctual currents, $n = 12$.

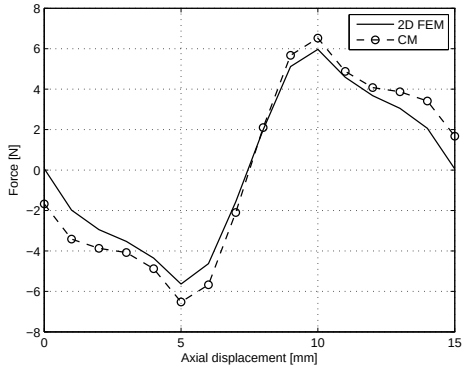

Fig. 8. Force for one tooth.

6. 3D-simulated model

Thanks to the periodicity in the machine it is enough to simulate only one pole pair. Periodic boundary conditions are put on the upper and the lower sides of the segment. These conditions require that the mesh on these two sides are exactly the same. It is because of this the simulated segment has to be taken in the middle between the two iron stacks. Alternatively, as it is done in this case, only one thin slice is taken of the neighboring pole. The reason for this lies only in simplicity of the modeling of the segment in the 3D-FEM software.

The simulated segment of the machine geometry is shown in figure 9.

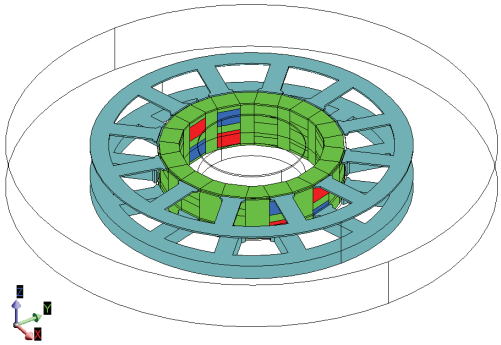

Fig. 9. 3D Simulated model.

Due to the boundary conditions, simulations with the time stepping were not possible. In order to perform the cogging force simulation a new model, with the magnet displacement, was simulated for each step.

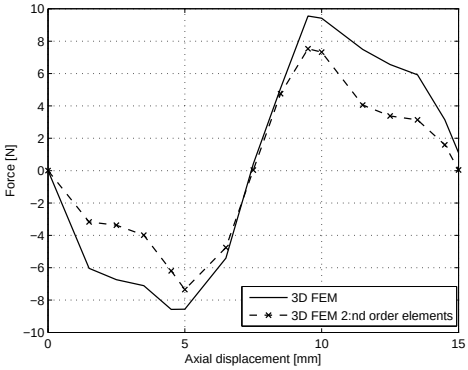

Fig. 10. 3D-simulated force for one phase magnets.

The simulated results are shown in figure 10.

Figure 10 shows results from the 3D-simulations only for one phase and one pole. There is clearly a difference between the 1:st and 2:nd order elements results. This indicates that the number of mesh elements generated should probably be increased.

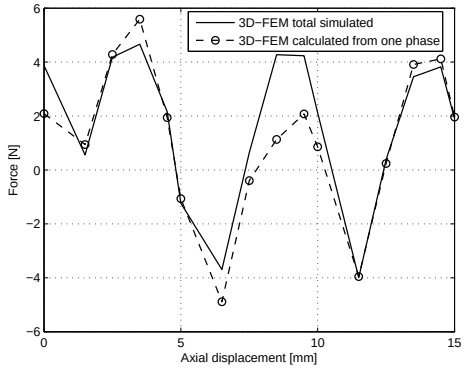

Fig. 11. 3D-simulated force for all phases and calculated results from 3D-FEM results for one phase.

Total results of the cogging force are obtained by shifting the one phase results by 120 electrical degrees in axial direction. The results are shown in figure 11. It can be seen that the correlation is acceptable. It should be mentioned that the simulation are performed only with 1:st order elements, and, as mentioned, 2:nd order or denser mesh is necessary. Hopefully even better agreement can then be achieved.

7. Conclusions

The CM method is a powerful tool to calculate the filed in a complex geometry. It is mainly used for the 2D analysis.

As can been seen from the figure the correlation between the simulated and calculated results is good, but not as good as expected. There are two reasons for this. The first is the number of the punctual currents that represents the magnet and the second is the mesh density in the simulated model. Increasing the number of punctual currents and increasing the mesh density around the air gap would probably result in better agreement.

However, the correlation between the 3D-FEM results and 2D-FEM results are not good enough. It can be seen that the results from 2D-FEM and CM calculations indicate a approximately 2-3 times bigger. At this stage no good explanation can be given for this cause. The validation of the results will be verified firs after the measurement on the prototype, shown in 12. Due to the lack of time the measurement were not performed at the moment this paper was written.

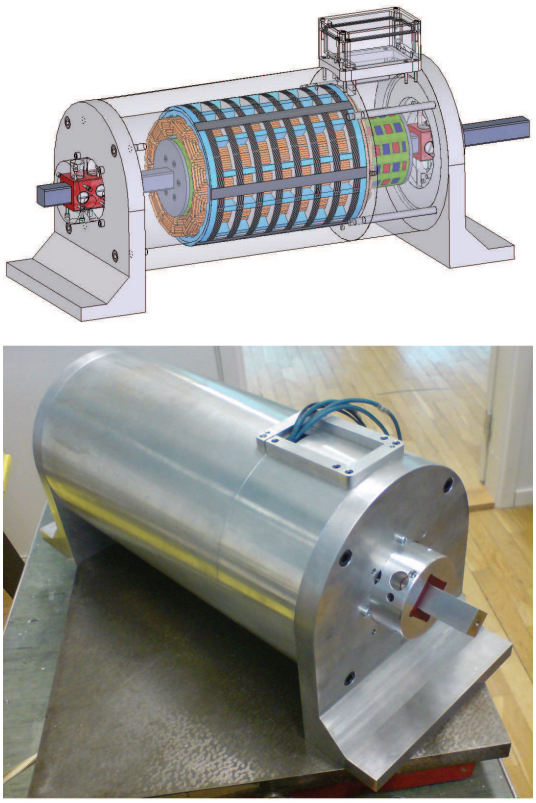

Fig. 12. Prototype of the novel linear TFM.

Acknowledgement

The authors would like to thank the European Commission for the financial support for this work.

References

[1] W. M. Arshad: *A Low-Leakage Linear Transverse-Flux Machine for a Free-Piston Generator*, Ph.D. Thesis, ISBN 91-7283-535-4, Royal Institute of Technology, Stockholm, 2003

[2] Z. Q. Zhu and D. Howe: *Analytical Prediction of Cogging Torque in Radial-field Permanent Magnet Brushless Motors*, IEEE Transactions on Magnetics, VOL. 28, NO. 2, March 1992

[3] M. Markovic, M. Jufer and Y. Perriard: *Determination of Tooth Cogging Force in a Hard-Disk Brushless DC Motor* , IEEE Transactions on Magnetics, VOL. 41, NO. 12, December 2005

[4] C. Sadarangani: *Electrical Machines, Design and Analysis of Induction and Permanent Magnet Motors*, ISBN 91-7170-627-5, KTH Hogskoletryckeriet, Stockholm, 2000

[5] A. Cosic,C. Sadarangani and F. Carlsson: *A novel concept of a Transverse Flux Linear Free-Piston Generator*,Linear Drives for Industry Applications (LDIA 2005), Kobe-Awaji, Japan, 2005

[6] E. P. Furlani : *Permanent Magnet and Electromechanical Devices Materials*, Academic Press, ISBN 0122699513, 2001